A novel cell response triggered by interphase centromere structural instability

Eric Morency,[1,2] Mirna Sabra,[1,2] Frédéric Catez,[1,2] Pascale Texier,[1,2] and Patrick Lomonte[1,2]

[1]Viral Silencing and Centromeric Instability Team, Université Lyon 1, Lyon F-69003, France
[2]Centre National de la Recherche Scientifique, Unité Mixte de Recherche 5534, Centre de Génétique Moléculaire et Cellulaire, Villeurbanne F-69622, France

Interphase centromeres are crucial domains for the proper assembly of kinetochores at the onset of mitosis. However, it is not known whether the centromere structure is under tight control during interphase. This study uses the peculiar property of the infected cell protein 0 of herpes simplex virus type 1 to induce centromeric structural damage, revealing a novel cell response triggered by centromere destabilization. It involves centromeric accumulation of the Cajal body–associated coilin and fibrillarin as well as the survival motor neuron proteins. The response, which we have termed interphase centromere damage response (iCDR), was observed in all tested human and mouse cells, indicative of a conserved mechanism. Knockdown cells for several constitutive centromere proteins have shown that the loss of centromeric protein B provokes the centromeric accumulation of coilin. We propose that the iCDR is part of a novel safeguard mechanism that is dedicated to maintaining interphase centromeres compatible with the correct assembly of kinetochores, microtubule binding, and completion of mitosis.

Introduction

Centromeres are specialized chromosome domains that are responsible for chromosome segregation during meiosis and mitosis. They assemble around repetitive DNA sequences in a complex structure that has yet to be fully elucidated. A simplistic view involves the division of this domain into two areas: the central core region or centromeric chromatin (Schueler and Sullivan, 2006) and the flanking heterochromatic regions, which are called pericentromeres. The protein composition of the central core region varies between interphase and mitosis. In this model, constitutive proteins are permanently associated with the centromere even during interphase, whereas facultative proteins are recruited only during mitosis to assemble the kinetochore, which is the site of microtubule attachment. As such, the central core region serves as the assembly platform for the kinetochore. A specific feature of the chromatin structure of the core centromere is that it contains interspersed blocks of nucleosomes that contain histone H3 and a histone H3 variant called centromeric protein (CENP) A in human cells (Blower et al., 2002). In addition to histones, six constitutive proteins named CENP-A, -B, -C, -H, -I, and hMis12 are known as the major components of the interphase centromeric chromatin. However, another set of 11 proteins associated with the CENP-A–containing nucleosomes or with the CENP-H–I complex has recently been described (Foltz et al., 2006; Okada et al., 2006).

Cajal bodies (CBs) are nuclear domains that were discovered in 1903 by the Spanish physiologist Santiago Ramón y Cajal (Gall, 2003). These bodies are concentrates of several proteins and small nuclear ribonucleoproteins (Matera and Shpargel, 2006). Among these proteins, coilin was described in the early 1990s as the major component of CBs (Raska et al., 1991), although its precise biological activity remains elusive. Orthologues of human coilin are known in many vertebrates, including the mouse (Tucker et al., 2000), *Xenopus laevis* (Tuma et al., 1993), *Danio rerio* (Tucker et al., 2000), *Arabidopsis thaliana* (Collier et al., 2006), and *Drosophila melanogaster* (Liu, J.L., and J.G. Gall, personal communication). Coilin is not strictly essential for mouse embryonic development, although a substantial reduction of viability has been observed in inbred homozygous embryos (Tucker et al., 2001). Coilin contains nuclear and nucleolar localization domains, an arginine-glycine (RG)–rich box, and an autointeraction domain that facilitates CB formation (Hebert and Matera, 2000). The formation of CBs depends, at least in part, on the autointeraction domain and on posttranslational modifications of coilin. Indeed, hyperphosphorylation considerably reduces the coilin autointeraction, which leads to CB disassembly during mitosis (Hebert and Matera, 2000; Shpargel et al., 2003).

Correspondence to Patrick Lomonte: lomonte@cgmc.univ-lyon1.fr

Abbreviations used in this paper: α-SAT; α-satellite; CB, Cajal body; CENP, centromeric protein; ChIP, chromatin immunoprecipitation; GAPDH, glyceraldehyde-3-phosphate dehydrogenase; HSV-1, herpes simplex virus type 1; iCDR, interphase centromere damage response; ICP0, infected cell protein 0; IF, immunofluorescence; PML, promyelocytic leukaemia; SMN, survival motor neuron; snRNA, small nuclear RNA; WB, Western blotting; wt, wild type.

The Journal of Cell Biology, Vol. 177, No. 5, June 04, 2007 757–768
http://www.jcb.org/cgi/doi/10.1083/jcb.200612107

The biological function of coilin within CBs remains mysterious, and its additional diffuse staining in the nucleoplasm has been proposed to be the mark of still unrevealed CB-independent activity (Matera and Frey, 1998).

Herpes simplex virus type 1 (HSV-1) infection of cultured cells induces the destabilization of centromeres during interphase, preventing the assembly of the kinetochore and the binding of microtubules during mitosis (Everett et al., 1999a). The factor responsible for this centromere destabilization is the viral protein infected cell protein 0 (ICP0). ICP0 is a RING finger nuclear protein with characterized E3 ubiquitin ligase activity (for review see Hagglund and Roizman, 2004). As soon as it enters the nucleus, ICP0 temporarily localizes to centromeres and induces the proteasomal degradation of CENP-A, -B, and -C (Everett et al., 1999a; Lomonte et al., 2001; Lomonte and Morency, 2007). Thus, ICP0-induced degradation of essential constitutive CENPs during interphase is likely to modify the structure of the central core region extensively, thereby preventing the assembly of the kinetochore. As a consequence, cells that express ICP0 just before entering mitosis are stalled in early mitosis and eventually suffer premature cell division without chromosomal segregation, leading to aneuploidy (Lomonte and Everett, 1999). Although the biological significance of ICP0-induced centromere destabilization is unclear, from the cellular viewpoint, ICP0 is of exceptional interest as a unique tool for studying centromere structure and the putative cell mechanisms implicated in centromere architectural maintenance. Indeed, although it is known that the cell uses kinetochore surveillance mechanisms during mitosis, such as the mitotic checkpoints (for review see Cleveland et al., 2003), it remains unknown whether the cell is able to detect centromeric structural defects in interphase.

In this study, using ICP0 as a tool, we reveal a previously unreported and unexpected cell response to human and mouse centromeres that have sustained structural modifications during interphase. This response is characterized by the accumulation at damaged centromeres of two CB proteins, coilin and fibrillarin, and one CB-associated gemini of CB (gems) nuclear domain protein, the survival motor neuron (SMN) protein. We show that this response does not implicate the entire CBs and/or gems. In addition, we confirm the physical association between coilin and centromere higher order type I α-satellite (α-SAT) DNA. Using siRNA against CENPs, we demonstrate that depletion

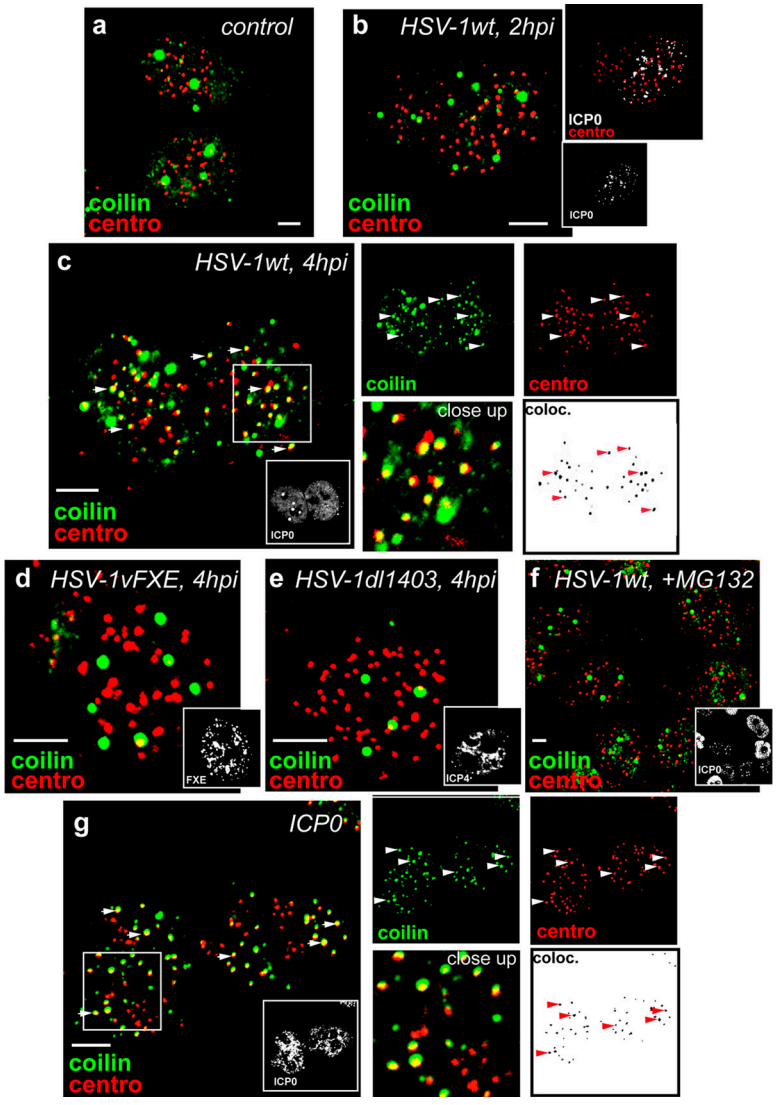

Figure 1. **Detection of a cellular response to damaged interphase centromeres.** (a) Coilin distribution in the CBs of control HeLa cells. (b) Coilin distribution in cells infected for 2 h with HSV-1 wt. The localization of ICP0 at centromeres is evidenced by the colocalization of white (ICP0) and red (centromere) dots. (c) Coilin distribution in cells infected for 4 h with HSV-1 wt. Centromeric coilin is clearly evident in the merged image as the colocalization of green (coilin) and red (centromere) dots. For a more representative view of the colocalization, the merged image was processed with the colocalization module of LSM 510 software (coloc.) so that all of the colocalized pixels appear black on a white background. ICP0 is present in the nucleoli (visible by counterstaining), as shown previously (Morency et al., 2005). (d and e) Coilin distribution in cells infected for 4 h with vFXE, a mutant virus that expresses a nonfunctional RING finger–deleted ICP0 protein, or by dl1403, a mutant virus that lacks ICP0 expression. (f) Coilin distribution in cells infected for 4 h with HSV-1 wt in the presence of the proteasome inhibitor MG132. (g) Detection of centromeric coilin in cells transfected with a plasmid that expresses ICP0. As in panel c, the merged image was processed with the colocalization module (coloc.) to show a more representative view of the colocalization. ICP0 and ICP4 (another viral protein that is detected when ICP0 is not present) serve as markers for the identification of infected or transfected cells. Centro, centromeres detected by huACA autoimmune serum. The arrowheads indicate several coilin signals that colocalize with centromeres. hpi, hours postinfection. Bars, 5 μm.

of CENP-B leads to the accumulation of coilin at centromeres. This confirms the existence of a cell response that is triggered by interphase centromere instability, for which we propose the term interphase centromere damage response (iCDR).

Results

Loss of constitutive CENPs from interphase centromeres induces a specific cell response

After our work on the ICP0-induced degradation of CENPs and the resulting destabilization of centromere structure, we decided to check whether and how cells were able to respond to centromere instability during interphase. Interphase HeLa cells were infected with HSV-1 wild-type (wt) virus and analyzed by immunostaining at 2 and 4 h after infection. As expected from our previous work, ICP0 transiently colocalized with centromeres at 2 h after infection but not at 4 h after infection (i.e., after degradation of the CENPs; compare ICP0 patterns in Fig. 1, b and c; insets; Everett et al., 1999b). At 4 h after infection (Fig. 1 c), ICP0 accumulated in large, visible foci inside the nucleoli as described previously (Morency et al., 2005). We found that at early stages of infection, the nuclear pattern of coilin underwent profound changes. Fig. 1 a shows noninfected cells in which coilin was localized in CBs. Infection by HSV-1 wt for 2 h did not substantially affect the coilin distribution (Fig. 1 b), whereas at 4 h after infection, coilin adopted a multidotted pattern in >90% of the infected cells (Fig. 1 c).

These coilin foci were more abundant and smaller than those that corresponded to CBs (0.2–0.5 μm for coilin foci vs. 1–1.2 μm for CBs in noninfected cells; compare coilin patterns in Fig. 1, a and c). Upon close examination, it was noticed that the nuclear distribution of these coilin dots looked very much like the pattern of immunostained centromeres. Therefore, we stained the latter together with coilin in ICP0-expressing cells; strikingly, most of the coilin foci indeed colocalized with centromeres (Fig. 1 c, yellow foci in the merged and magnified images). As the centromeric localizations of ICP0 and coilin were temporally separated (2 vs. 4 h after infection), the accumulation of coilin at centromeres is unlikely to be a consequence of an interaction with ICP0. Collectively, these data suggested that coilin accumulates at centromeres as a consequence of ICP0 activity on centromeres. To verify this notion, cells were infected with either the vFXE virus, which expresses the nonfunctional ICP0 RING finger mutant FXE, or the ICP0-null mutant dl1403, whose infection is detectable by ICP4 viral protein staining. We found that infection with these viruses did not induce coilin redistribution (Fig. 1, d and e).

ICP0 has E3 ubiquitin ligase activity that is associated with its RING finger domain. This activity is responsible for the induction of degradation via the proteasome of CENPs, which can lead to the destabilization of interphase centromeres and to defects in kinetochore assembly (Everett et al., 1999a). To verify the implication of proteasome activity in ICP0-induced coilin accumulation at centromeres, cells were infected with the HSV-1 wt virus in the presence of the proteasomal inhibitor MG132 or DMSO alone (unpublished data). In the presence of MG132, HSV-1 wt no longer induced the accumulation of coilin at centromeres (Fig. 1 f). These data suggest that there is a strong correlation between ICP0- and proteasomal-induced protein degradation (and probably CENP degradation) and the accumulation of coilin at centromeres.

Finally, to exclude any effect of the infection, we verified that transfected cells that expressed ICP0 (Fig. 1 g) but not those that expressed FXE (not depicted) showed a centromeric accumulation of coilin similar to HSV-1 wt–infected cells. As expected, 100% of the ICP0-expressing cells showed centromeric coilin. Note that during the course of these experiments, coilin colocalization with centromeres was never seen in mitotic cells. In conclusion, the aforementioned results demonstrate (1) the existence of a cell response that is triggered by the ICP0-induced structural damage of interphase centromeres (i.e., the iCDR) and (2) that coilin is implicated in the iCDR. These observations strongly suggest a role for coilin in a mechanism that is dedicated to the detection and/or repair of unstable interphase centromeric structures.

Centromeric coilin interacts with centromeric, chromatin-specific higher order type I α-SAT DNA

To determine whether coilin physically interacts with the central core region, we performed chromatin immunoprecipitation

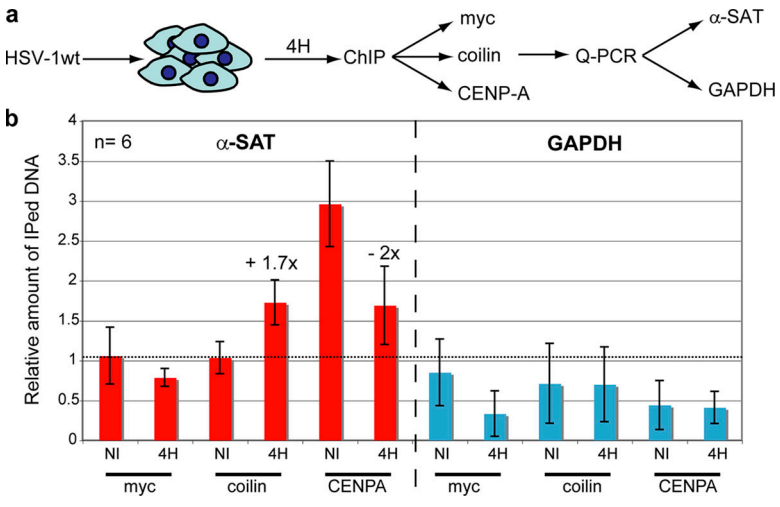

Figure 2. **Coilin interacts with centromeric type I α-SAT DNA.** (a) Noninfected HeLa cells (NI) or HeLa cells infected for 4 h (4H) with HSV-1 wt were used for ChIP and quantitative PCR (Q-PCR) assays. The ChIP assay was performed using standard procedures with the following antibodies: (1) anticoilin mAb to detect specific coilin–alphoid DNA interactions; (2) anti–CENP-A mAb as a positive control because this protein is depleted from the centromeres of infected cells (Lomonte et al., 2001); and (3) anti-myc tag mAb as a negative control for nonspecific alphoid DNA binding. The levels of centromeric α-SAT DNA and GAPDH DNA in the precipitated DNA were measured by quantitative PCR. A coverslip was added to each Petri dish to verify (by IF) coilin accumulation in and CENP-A depletion from centromeres at 4 h after infection (not depicted). (b) DNA samples immunoprecipitated with the different antibodies were quantified by real-time PCR using specific primers. Red bars show precipitated α-SAT DNA, and blue bars show precipitated GAPDH DNA. The data represent the ratios between the input and precipitated DNAs. The horizontal dotted line marks the limit of the background signal. The values and error bars are derived from six independent experiments. Error bars indicate mean ± SD.

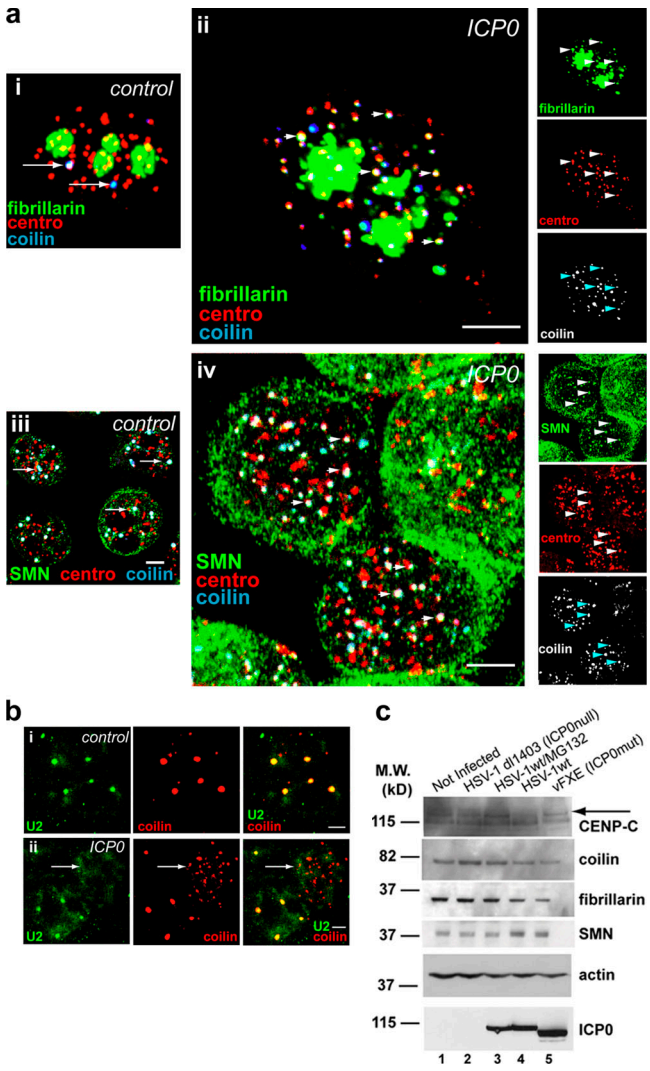

Figure 3. **Fibrillarin and SMN but not CB-associated U2 snRNA accumulate at damaged centromeres.** HeLa cells were either not transfected (control) or were transfected with an ICP0-expressing plasmid (ICP0) before performing IF or immuno-RNA FISH assays to detect the distribution of CB- and gem-associated proteins and RNAs. Cells that expressed ICP0 were detected by the particular centromeric coilin multidotted pattern described in Fig. 1. (a) IF detection of fibrillarin and SMN. In control cells, fibrillarin and SMN colocalize with coilin in the CBs (arrows in i and iii). Fibrillarin is also present in the nucleoli (large green areas). In ICP0-expressing cells, both proteins show a multidotted pattern similar to that of coilin, with which they colocalize at centromeres (arrowheads in ii and iv). Centro, centromeres detected by the huACA autoimmune serum. (b) Immuno-RNA FISH detection of U2 snRNA. (i) Control cells show a general nucleoplasmic staining for U2, with dense foci colocalizing with coilin. (ii) ICP0-expressing cells show the particular multidotted centromeric coilin without colocalizing U2 foci. The arrows point to a cell with multidotted centromeric coilin in which the classic CB-associated U2 pattern has disappeared. (c) ICP0 does not induce the proteasomal degradation of coilin, fibrillarin, or SMN. HeLa cells were either not infected (lane 1) or infected with virus HSV-1 wt in the presence (lane 3) or absence (lane 4) of the proteasome inhibitor MG132, dl1403 (ICP0 null; lane 2), or vFXE (ICP0 mutant that is 44 amino acids shorter than the full-length ICP0; lane 5) for 6 h. 40-μg aliquots of total protein were loaded in each lane to perform WB for the detection of CENP-C (positive control), coilin, fibrillarin, SMN, ICP0, and actin as the loading control. The arrow points to the CENP-C signal. Bars, 5 μm.

(ChIP) assays with HSV-1 wt–infected cells (Fig. 2 a) and looked for the association of coilin with centromeric, chromatin-specific higher order type I α-SAT DNA. In each case, we compared the ChIP of noninfected cells with that of cells at 4 h after infection (i.e., the time point at which coilin was found to have accumulated at centromeres; Fig. 1 c). The method and results were validated using an anti–CENP-A antibody as a control. Indeed, as expected, we observed a major decrease in the amount of CENP-A associated with type I α-SAT DNA as a consequence of ICP0-induced CENP-A degradation. We then tested an anticoilin antibody in parallel with the anti–CENP-A and anti-myc antibodies, with the latter being used as a nonspecific control (Fig. 2 b). In each experiment, a single batch of chromatin was split into three aliquots, one for each antibody, and the three ChIPs were performed simultaneously.

The results obtained (Fig. 2 b, left) show that more coilin is associated with α-SAT DNA at 4 h after infection compared with noninfected cells, whereas less CENP-A is present at 4 h after infection. In these experiments, the amount of α-SAT DNA associated with the anti-myc control antibody did not notably change. Considering that the 4-h postinfection CENP-A was undetectable at centromeres by immunofluorescence (IF) and almost completely degraded, as shown by Western blotting (WB; Lomonte et al., 2001), a twofold decrease in the amount of α-SAT DNA retrieved ($P < 0.05$) with CENP-A can be regarded as representative of a major effect. In this context, the 1.7-fold increase in α-SAT DNA retrieved with coilin ($P < 0.05$) is suggestive of a significant increase in coilin levels at centromeres, which fits with our aforementioned results (Fig. 1). The DNA of the housekeeping gene *glyceraldehyde-3-phosphate dehydrogenase* (*GAPDH*) was measured to control for binding of the anticoilin and anti–CENP-A antibodies to unrelated DNA, and, as expected, no enrichment of coilin was noted (Fig. 2 b, right). From these data, we conclude that ICP0-induced centromere destabilization results in a physical interaction between coilin and centromeric DNA.

Fibrillarin and SMN also accumulate at damaged interphase centromeres

A major issue in the biology of nuclear domains is whether the entire domain is involved in a process or only some components thereof. Thus, there was a need to determine whether components of CBs other than coilin also accumulate at damaged centromeres and, if so, whether whole CB domains are associated with centromeres in ICP0-expressing cells. In addition to coilin, CBs concentrate several small noncoding RNAs as well as an array of proteins, all of which are more or less implicated in transcription (Gall, 2001). Apart from fibrillarin, no other tested CB-associated protein exhibits centromeric accumulation in ICP0-expressing cells (Fig. 3 a, i and ii; Fig. 4, a–e; and Table I). Fibrillarin is one of the most abundant proteins in the fibrillar regions of the nucleolus. It is conserved from yeast to humans and is essential for early development in the mouse, being a catalyst of preribosomal RNA methylation (Omer et al., 2002; Newton et al., 2003). Because CBs also contain RNAs, immuno-RNA FISH assays were performed to analyze the pattern of the major CB-associated U2 small nuclear

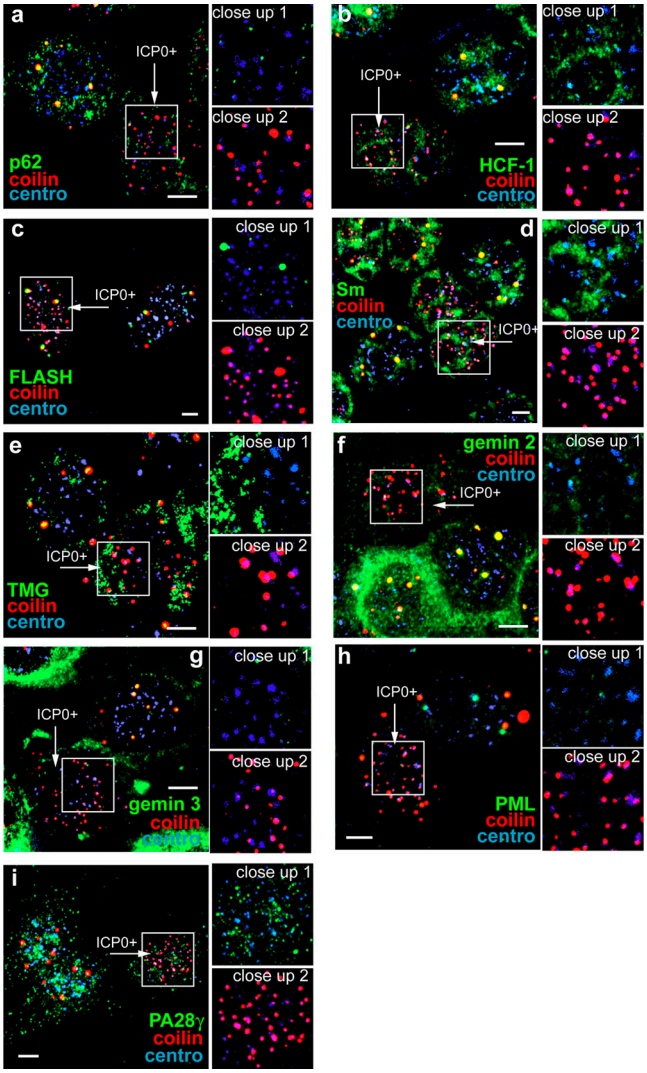

Figure 4. **Other CB and gem proteins do not accumulate at damaged centromeres.** HeLa cells were transfected with an ICP0-expressing plasmid before IF assays to detect the distribution of CB- and gem-associated proteins. Cells that expressed ICP0 (ICP0+; arrows) were detected by the particular centromeric coilin multidotted pattern described in Fig. 1. (a–e) CB-associated markers p62, HCF-1, FLASH, Sm, and TMG. (f and g) The gem-associated markers gemin 2 and 3. (h) PML body marker protein PML. (i) UV-C stress-induced coilin-interacting protein PA28γ. In control cells, all of the CB and gem markers colocalize with coilin in CBs (yellow dots in the merged images). In ICP0-expressing cells, none of these markers colocalize to centromeres (close up 1), as does coilin (close up 2). The PML pattern is shown as a control for the behavior of another nuclear domain-associated protein. PML is known to be degraded in an ICP0- and proteasomal-dependent manner in ICP0-expressing cells (Everett et al., 1998). The PA28γ pattern was analyzed because it shows colocalization with coilin in UV-C–treated cells (Cioce et al., 2006). Centro, centromeres detected by the huACA autoimmune serum. Bars, 5 μm.

RNA (snRNA) in ICP0-expressing cells. No centromeric accumulation of U2 was detected (Fig. 3 b, i and ii). In addition, antibodies raised against both the 5′-terminal caps of the snRNAs and the snRNA-binding Sm proteins did not show any centromeric signals in ICP0-expressing cells (Fig. 4, d and e; and Table I). Collectively, these data indicate that only some components of the CBs, such as coilin and fibrillarin, accumulate at damaged centromeres.

Table I. **Accumulations of CB and gem components at damaged interphase centromeres**

CB	Accumulation at centromeres
Protein component	
Coilin	Yes
Fibrillarin	Yes
Sm	No
p62 (TFIIH subunit)	No
HCF-1 (host cell factor 1)	No
FLASH	No
RNA component	
U2 (snRNA)[a]	No
TMG-cap[b]	No
Gems	
SMN	Yes
Gemin 2	No
Gemin 3	No
Other proteins	
PML	No
PA28γ	No

Sm proteins bind to snRNPs and become concentrated in CBs. FLICE-associated huge protein (FLASH) has recently been described as a component of CBs (Barcaroli et al., 2006). PML is the major component of the nuclear bodies, which are called PML nuclear bodies, ND10, or PML oncogenic domains. PML is degraded in an ICP0- and proteasomal-dependent manner (Everett et al., 1998). Under certain circumstances, PML bodies can be connected to centromeres in the G2 phase (Everett et al., 1999b; Luciani et al., 2006). PA28γ (proteasome activator γ) has recently been shown to colocalize and associate with coilin in UV-C–treated cells (Cioce et al., 2006).
[a]As shown by immuno-RNA FISH assays (see Fig. 3 b, ii).
[b]As detected by the 5′-2,2,7-trimethylguanosine (TMG) antibody, which recognizes TMG-capped snRNAs.

In the cell nucleus, gems were originally defined as CB-associated domains on the basis of IF staining with antibodies against the SMN protein (Liu and Dreyfuss, 1996). This protein is the product of the *SMN* gene, whose loss of function mutations are responsible for the severe inherited disorder spinal muscular atrophy, one of the major genetic causes of infant mortality (Lefebvre et al., 1995). We decided to check the patterns of gem-associated proteins in ICP0-expressing cells. Three gem proteins, SMN, gemin 2, and gemin 3, were tested and showed foci that colocalized with CBs in control cells (Fig. 3 a, iii; arrows for SMN; and Fig. 4, f and g; gemin 2 and 3). In ICP0-expressing cells, SMN but not gemin 2 or 3 was detected in numerous small foci that, similar to coilin and fibrillarin, colocalized with centromeres (Fig. 3 a, iv; arrowheads; Fig. 4, f and g; and Table I). As was the case for coilin, 100% of the ICP0-expressing cells showed centromeric fibrillarin and SMN.

The aforementioned experiments suggest that neither coilin, fibrillarin, nor SMN is degraded in ICP0-expressing cells. To confirm this point, cells were infected with HSV-1 wt in the presence or absence of the proteasome inhibitor MG132, vFXE, or dl1403 viruses at a multiplicity of infection of 10 (100% of the cells infected; Fig. 3 c). Coilin, fibrillarin, and SMN did not sustain ICP0-induced degradation.

These data rule out a putative relocalization of the entire CB and/or gem to damaged centromeres and strongly suggest the existence of a specific subset of nuclear proteins (containing at least coilin, fibrillarin, and SMN) that accumulates in response to centromere damage. Therefore, coilin, fibrillarin, and SMN

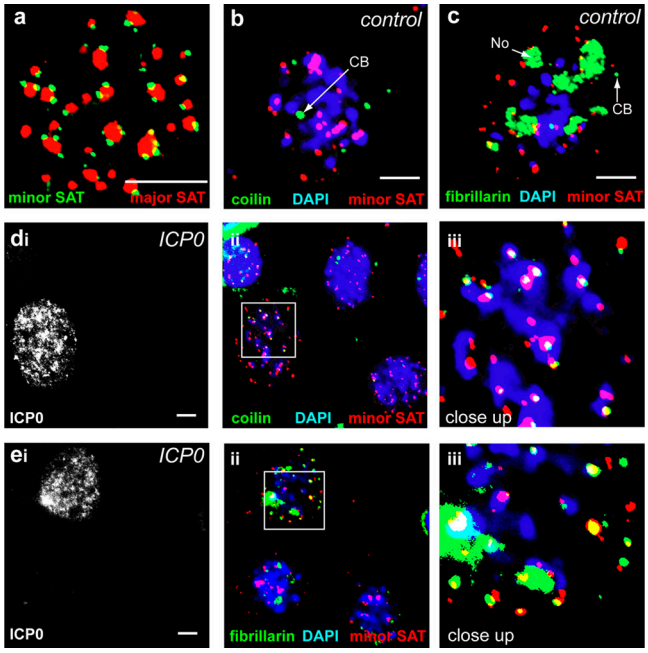

Figure 5. **The iCDR is conserved in mouse cells.** Mouse NIH3T3 cells were transfected with the ICP0-expressing plasmid before immuno-DNA FISH assays for the detection of coilin, fibrillarin, and centromere minor satellite sequences. (a) FISH of noninfected cells for the detection of pericentromere and central core regions using probes against the major (major SAT; red) and minor (minor SAT; green) DNA repeat sequences, respectively. The pattern corresponds to that described previously (Guenatri et al., 2004). (b and c) Control cells labeled for coilin or fibrillarin, minor satellite repeats, and pericentromeres (DAPI). CB, Cajal body; No, nucleolus. (d) The same area of cells transfected and stained for the detection of ICP0 (i), coilin, minor satellite repeats, and pericentromeres (ii). Coilin is present in the multidots in the ICP0-positive cell, similar to its behavior in human cells. Several of these coilin dots colocalize with minor satellite repeats. (iii) Magnification of the ICP0-expressing cell shown in the boxed area. (e) The same area of cells transfected and stained for the detection of ICP0 (i) and fibrillarin, minor satellite repeats, and pericentromeres (ii). Fibrillarin is present in the multidots in ICP0-positive cells, similar to its behavior in human cells. Several of these fibrillarin dots colocalize with minor satellite repeats. (iii) Magnification of the ICP0-expressing cell shown in the boxed area. Bars, 10 μm.

most likely have activities associated with damaged centromeres in addition to their nuclear domain-associated functions.

The iCDR is conserved in mouse cells

We observed the iCDR in additional human cell lines of various origins (e.g., breast carcinoma [T47D], colon carcinoma [SW480, HCT116, and HT29], and skin cancer [HaCaT]) as well as in primary keratinocyte cells. To determine whether this response is conserved in other species, the centromeric accumulations of coilin, fibrillarin, and SMN were analyzed in mouse NIH3T3 cells, which express ICP0. In mouse nuclei, chromosomes are distributed in clusters, and pericentromeric heterochromatin forms chromocenters that can be visualized by DAPI staining. The DNA sequences of the central core and pericentromere regions are based on two different types of DNA repeat, called minor and major satellites, respectively. These two domains are spatially separated and are clearly distinguishable by in situ hybridization (Fig. 5 a; Pietras et al., 1983; Guenatri et al., 2004). We performed immuno-DNA FISH assays on ICP0-expressing cells to detect ICP0 (Fig. 5, d and e), minor satellite DNA, and coilin or fibrillarin (the anti-SMN mAb does not work on mouse cells). In the absence of ICP0, coilin and fibrillarin showed the same patterns in the mouse as in human cells (i.e., present in CBs and/or nucleoli; Fig. 5, b and c). In ICP0-expressing cells, coilin (Fig. 5 d, i–iii) and fibrillarin (Fig. 5 e, i–iii) showed a multidotted pattern that was similar to the pattern in human cells. These dots clearly colocalized with the minor satellite signals and, thus, with the central core region of the centromere. These data show that the iCDR is conserved in mammalian cells, at least between humans and mice, and is not an artifact of a single cell line.

The iCDR is not induced by DNA breaks

A recent study has described the effect of UV-C irradiation on CB fragmentation (Cioce and Lamond, 2005). Consequently, coilin showed a change of pattern and increased interaction with PA28γ (proteasome activator subunit γ), a protein that is implicated in some aspects of proteasome activity in vitro (Wilk et al., 2000). This interaction resulted in the colocalization of coilin and PA28γ in UV-C–treated cells. Because UV light irradiation induces DNA breaks, the putative participation of coilin in a mechanism that is designed to resolve such damage to DNA has to be considered. Therefore, we investigated whether the response to ICP0-induced damaged centromeres implicated protein complexes involved in DNA break repair. PA28γ did not colocalize with coilin at the centromeres of ICP0-expressing cells (Fig. 4 i and Table I). Likewise, several proteins involved in single- or double-strand DNA break repair pathways (including nucleotide excision, base excision, and double-strand break repair) did not relocalize at the damaged centromeres in ICP0-expressing cells (Fig. 6, a–g; and Table II). Given that irradiation of HeLa cells with γ rays (from 2 to 10 Gy) does not provoke CB fragmentation (unpublished data) and that ICP0 is not known to provoke DNA breaks, these data do not support the accumulation of centromeric coilin, fibrillarin, and SMN as part of a putative DNA damage response–associated mechanism with activity in resolving DNA breaks.

The loss of CENP-B triggers coilin accumulation at centromeres

The aforementioned results demonstrate that ICP0 provokes the accumulation of at least three proteins at damaged centromeres. However, one could argue that the accumulations of coilin, fibrillarin, and SMN at centromeres are caused by an as of yet unknown activity of ICP0 and are not a direct result of CENP degradation. Therefore, we induced centromere destabilization independently of ICP0 using siRNAs that target the mRNAs of CENP-A, -B, and -C, the three known CENPs that are degraded in an ICP0-dependent manner. We verified by IF (Fig. 7 a) and WB (Fig. 7 b) the effects of the siRNAs on the stability of the targeted proteins. HeLa cells were transfected with single-type siRNAs or a mixture of two or three siRNAs, and the cells were then immunostained to detect (1) decreases in the amounts of the targeted proteins from centromeres and (2) centromeric accumulations of coilin, fibrillarin, and SMN. Cells with multidotted coilin, fibrillarin, or SMN, which were representative of the accumulations of these proteins at

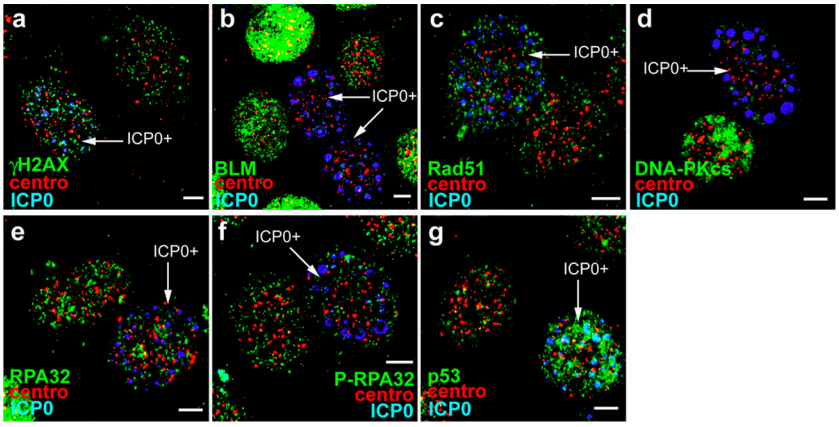

Figure 6. **Proteins involved in DNA break repair complexes do not accumulate at damaged centromeres.** HeLa cells were transfected with the ICP0-expressing plasmid before IF assays. The distributions of several proteins involved in DNA break repair mechanisms with regard to the centromeres were analyzed in ICP0-expressing cells (ICP0+; arrows). (a) γH2AX; (b) BLM; (c) Rad51; (d) the catalytic subunit of DNA-PK (DNA-PKcs); (e) RPA32; (f) P-RPA32; (g) p53. Each panel contains at least one control cell and one cell that expresses ICP0. The signals for BLM (b) and DNA-PKcs (d) show important decreases in ICP0-expressing cells. The increase in the p53 signal in ICP0-expressing cells (g) is not significant. Centro, centromeres detected by the huACA autoimmune serum. Bars, 5 μm.

centromeres, were counted in several experiments that were performed independently. A scrambled sequence siRNA never had any effect on the coilin, fibrillarin, or SMN patterns. Similarly, none of the three CENP siRNAs was able to induce multidotted fibrillarin or SMN in a manner similar to ICP0 even when used in combination (unpublished data). Interestingly, coilin showed a multidotted pattern in a small proportion (~5%) of cells that were treated with the CENP-A or -C siRNA and in a large proportion (~30%) of cells that were treated with the CENP-B siRNA (Fig. 7 c).

We confirmed by IF that the multidotted coilin colocalized with centromeres (Fig. 7 d). To show a more representative view of the colocalization, the merged images were processed, as in Fig. 1 (c and g) with the colocalization module of the LSM 510 software, so that all of the colocalized pixels appeared black on a white background (Fig. 7 d, right column). CENP-A colocalization with huACA staining was used as a positive control (Fig. 7 d, i). A large proportion of coilin colocalized with centromeres in ICP0-expressing cells (Fig. 7 d, iii) as well as in CENP-B siRNA-treated cells (Fig. 7 d, iv). Much fewer black spots were visible in the few CENP-A (or CENP-C; not depicted) siRNA-treated cells that showed multidotted coilin (Fig. 7 d, v), and almost no black spots were seen in the scrambled sequence siRNA-treated cells (Fig. 7 d, ii). In addition, the proportion of centromeres that colocalized with coilin was determined (Fig. 7 d, right column; numbers in parentheses). Several images were scanned in each experiment (Fig. 7 d, i–v) to determine a mean colocalization coefficient between centromeres and coilin. The coefficient for CENP-A colocalization with centromeres was arbitrarily fixed at 1. The colocalization coefficient in untreated cells or cells transfected with the scrambled sequence siRNA was very low, with a value of 0.046. Cells that were treated with the CENP-A (or CENP-C) siRNA showed a fivefold increase in the colocalization coefficient (0.28). ICP0-expressing cells and CENP-B siRNA-treated cells gave the highest coefficient (0.45) for coilin/centromere colocalization, with a 10-fold increase compared with the normal situation. The specificity of the accumulation of coilin at centromeres that lacked CENP-B and, to a lesser extent, CENP-A and -C renders an off-target effect of the siRNAs highly unlikely. However, we tested another siRNA against CENP-B and obtained similar results (unpublished data). These results confirm that the iCDR is triggered as a direct consequence of the loss of some constitutive CENPs and, thus, by the instability of the centromere structure.

Discussion

In this study, we took advantage of the effect of the ICP0 protein on the destabilization of centromere structures to investigate whether cells survive and adapt to such dramatic modifications at domains of major importance for their viability. We reveal a novel cellular response, named iCDR, suggesting the existence of mechanisms dedicated to dealing with structural damage to centromeres during interphase (i.e., before the onset of mitosis). We also describe a role for coilin in the iCDR, which implicates two other proteins, fibrillarin and SMN. In addition, the fact that several human cell lines and mouse cells manifest a similar response suggests a general mechanism that is likely to be conserved, at least in mammals.

Table II. **Involvement of DNA break repair mechanisms in the cellular response to damaged interphase centromeres**

Proteins involved in DNA break repair[a]	Accumulation at centromeres in ICP0-expressing cells	Remarks
γ-H2AX	No	NA
BLM	No	NA
Rad51	No	NA
DNA-PKcs	No	Degraded in an ICP0- and proteasomal-dependent manner[b]
RPA32	No	NA
P-RPA32	No	NA
p53	No	NA
p62 (TFIIH)	No	CB-associated protein (see Table I and Fig. 3)

γ-H2AX is rapidly phosphorylated on S139 in response to DNA damage. BLM is a helicase from the recQ subfamily that is involved in the cellular response to DNA damage and stalled replication forks. It participates with Rad51 in homologous recombination. DNA-PK plays a central role in the nonhomol ogous end-joining DNA pathway. DNA-PKcs is the catalytic subunit of DNA-PK. Replication protein A (RPA) is a single-stranded DNA-binding protein that is composed of three subunits of 70, 32, and 14 kD. RPA is essential for the recombination and DNA repair pathways. RPA32 becomes hyperphosphorylated on S4 and S8 in response to DNA damage. p62 is a core subunit of the transcriptional/repair factor TFIIH, which is involved in the nucleotide excision repair pathway. NA, not applicable.
[a]Nucleotide excision, base excision, and double-strand breaks.
[b]As shown previously (Parkinson et al., 1999).

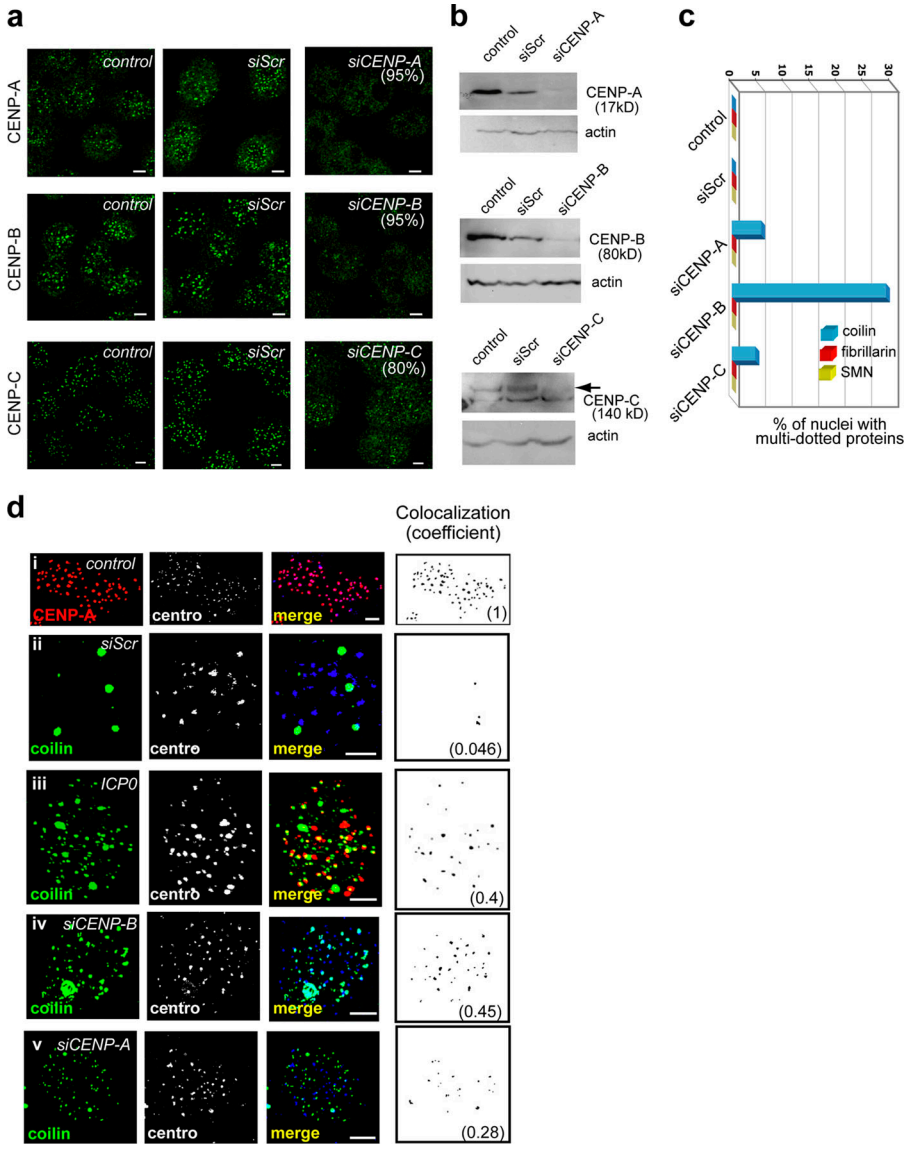

Figure 7. **CENP-B depletion induces coilin accumulation at damaged centromeres.** (a and b) To validate the efficiency of the siRNAs, HeLa cells were either not transfected (control) or were transfected with a scrambled sequence siRNA (siScr) or siRNAs against CENP-A, -B, or -C. Decreases in the CENP-A, -B, and -C signals were detected by IF (a) or WB (b) using the appropriate antibodies. The numbers in parentheses in panel a are the estimated percentages of cells that showed a substantial decrease in the protein signal. The arrow in panel b points to the CENP-C signal. (c) Counting of the nuclei with multidotted coilin, fibrillarin, or SMN in HeLa cells knocked down for CENP-A, -B, or -C. In total, ~800 cells were analyzed for each protein from several independently performed experiments. The graph shows the percentage of nuclei with multidotted proteins. (d) IF showing protein colocalization with centromeres in HeLa cells not treated (i), expressing ICP0 (iii), or transfected with siRNAs (ii, iv, and v). Each pixel resulting from the colocalization of coilin (ii–v) or CENP-A (i) with centromeres viewed in the merged images is visualized by black spots using the colocalization module of LSM 510 software. The numbers in parentheses represent the calculated colocalization coefficients (mean). The coefficient for CENP-A colocalization to centromeres is arbitrarily fixed at 1. Centro, centromeres detected by the huACA autoimmune serum. Bars, 5 μm.

Importantly, our data from cells knocked down for CENP proteins confirm the existence of a cellular response that is triggered directly by structural modifications to centromeres. Although efficient for coilin, the single and combined siRNAs were, unlike ICP0, ineffective in stimulating fibrillarin and SMN. Therefore, the centromeric accumulations of fibrillarin and SMN are probably induced by more severe damage than that arising from the absence of CENP-A, -B, or -C or by the absence of other CENPs. Interphase centromeres are complex structures organized into multisubunit protein domains that are associated partly with the CENP-H–I complex and partly with the centromere-specific CENP-A–containing nucleosomes in the distal (CENP-A nucleosome distal) and proximal (CENP-A nucleosome-associated complex) layers (Foltz et al., 2006; Okada et al., 2006). In light of our results, these data are informative in two respects. First, to engineer the collapse of the entire centromeric structure using CENP-directed siRNAs, it is necessary to affect more than one protein. Second, it is anticipated that ICP0 induces the proteasomal degradation of more CENPs than the individual CENP-A, -B, and -C proteins. Therefore, a simple explanation for the differential centromeric accumulations of coilin, fibrillarin, and SMN seen in this study may be the levels of damage caused to the different layers of CENPs.

Coilin accumulation at damaged centromeres is induced by CENP-B depletion, which suggests that the absence of CENP-B, unlike the absence of CENP-A and -C, is sufficient to trigger the response. CENP-B is a DNA-binding protein that has been implicated by in vitro studies in the positioning of nucleosomes (Yoda et al., 1998; Tanaka et al., 2005). It is unclear whether there is an absolute requirement for CENP-B for the preservation of centromere structure and function, as knockout mice for CENP-B are viable (Hudson et al., 1998; Kapoor et al., 1998; Perez-Castro et al., 1998) and CENP-B is essential for the de novo formation of centromeres, control of the epigenetic state of centromeric chromatin, and assembly of CENP-A (Masumoto, H., personal communication; Ohzeki et al., 2002). In any case, CENP-B is highly conserved in higher eukaryotes, which does not fit with the absence of major phenotype reported

in the *cenpB*$^{-/-}$ mice studies (Hudson et al., 1998; Kapoor et al., 1998; Perez-Castro et al., 1998). The fact is that in the particular context of mouse cells, centromeres are stable and functional even if the *cenpB* gene is missing. One explanation is that in *cenpB*$^{-/-}$ mice, the centromere structures could have acquired a CENP-B–independent equilibrium that is epigenetically transmissible. This situation is not quite the same as the one described in our present study, in which we hypothesize the rapid disruption of the equilibrium of the centromere structure by the rapid degradation of CENPs. In this regard, we investigated the coilin and fibrillarin distributions in untreated (not expressing ICP0 and not transfected with CENP siRNAs) *cenpB*$^{-/-}$ mouse embryonic fibroblast cells derived from CENP-B knockout mice and did not detect any accumulations of these proteins at centromeres (unpublished data).

We know that the accumulation of coilin and fibrillarin at damaged centromeres occurs in ICP0-expressing mouse NIH3T3 cells (this study) and normal mouse embryonic fibroblast cells (unpublished data). Therefore, the absence of the accumulation of these proteins at the centromeres of steady-state *cenpB*$^{-/-}$ mouse embryonic fibroblast cells suggests that the centromeric coilin, fibrillarin, and SMN proteins do not act as part of a putative structural complex that replaces the missing proteins but rather as a response of the cell to dramatic modifications of the centromere structure at a given time point. Centromeres possess a very specific organization of their chromatin compared with noncentromeric chromatin, and, thus, they are likely to concentrate unique cellular processes. Our data showing that ICP0-expressing cells lack centromeric accumulations of proteins implicated in DNA break repair mechanisms do not favor the hypothesis of DNA lesions as a direct consequence of the accumulations of centromeric coilin, fibrillarin, and SMN. Therefore, it is likely that the modification of centromere structure itself is responsible for triggering the iCDR. Interestingly, two out of the three known CENP targets of ICP0, CENP-A and -B, are established chromatin-related proteins. This raises the question as to whether the recruitment of centromeric coilin, fibrillarin, and SMN is initiated by the abnormal protein content of the centromere and/or by the abnormal chromatin structure.

On the basis of the data in the literature, it is difficult to come up with a convincing explanation for the interactions of coilin, fibrillarin, and SMN with damaged centromeres. First, this association was unexpected. Second, there is a general lack of information concerning the architecture of the central core centromere, particularly during interphase. However, coilin, fibrillarin, SMN, and centromeres may be linked by RNAs, especially small noncoding RNAs. Indeed, coilin, fibrillarin, and SMN are components of nuclear bodies, CBs, and gems, whose best-characterized functions remain the maturation of small noncoding RNAs that are implicated in the processing of larger transcripts. The association of small RNAs through the RNA interference mechanism with the epigenetic modifications of centromeric heterochromatin is now well documented, particularly in the yeast *Schizosaccharomyces pombe* (for reviews see Pidoux and Allshire, 2005; Verdel and Moazed, 2005). Importantly, this RNAi-dependent heterochromatinization is directly linked to transcriptional activity in the pericentromeric heterochromatin. Although the existence of a similar mechanism in higher eukaryotes has not yet been demonstrated, it is clear that centromeric heterochromatin–associated transcriptional activity is conserved at least in humans, maize, rice, and chickens (Saffery et al., 2003; Fukagawa et al., 2004; Topp et al., 2004; Zhang et al., 2005). Moreover, recent studies have shown that transcription and small RNAs can participate in the architecture and function of centromeres in murine cells (Maison et al., 2002; Bouzinba-Segard et al., 2006). From these data, it is tempting to speculate that the presence of coilin, fibrillarin, and SMN at damaged centromeres reflects the involvement of RNAs in maintaining the centromeric chromatin structure. Future studies should provide new information that is relevant to this hypothesis.

At the molecular level, we anticipate a close link between the iCDR and the need to reform a functional centromere structure that has been accidentally damaged during interphase. This response could trigger a mechanism that eventually results in the reformation of a fully functional prekinetochore. This inevitably raises questions as to the consequences of centromere instability for general chromosomal instabilities that result in aneuploidy and cancer development (Jallepalli and Lengauer, 2001). Several types of genetic alteration are responsible for chromosomal instabilities, including those that affect kinetochore functions (Bharadwaj and Yu, 2004). Although there is a clear need for correct kinetochore structures to prevent chromosomal instabilities, not much is known concerning the capacities of interphase centromeres to serve as platforms for kinetochore nucleation. If interphase centromeres are unable to build functional kinetochores as a result of structural problems, it is likely that the mitotic spindle checkpoint will be weakened and its activity bypassed, forcing mitosis and provoking aneuploidy (for review see Rieder and Maiato, 2004). This is precisely what has been described in a recent study of late embryonic development in *Drosophila cid/cenp-A*–null mutants (Blower et al., 2006). Therefore, it is reasonable to propose the existence of a cellular response that acts as a sensor mechanism to signal the emergence of structural problems to interphase centromeres.

In retrospect, it is not surprising that cells are sensitive to defects at interphase centromeres considering the major roles of these genetic loci. To date, it has been unknown whether cells have developed mechanisms during interphase to check the functionalities of these structures. Our present results clearly show that this is probably the case, and they raise questions as to the existence of pathways that are committed to sensing, signaling, and repairing centromeres before the cell enters mitosis. In this framework, future studies will need to address the importance and functions of proteins, such as coilin, fibrillarin, SMN, and other proteins, in these types of pathways.

Materials and methods

Cell lines, plasmids, and viruses

HeLa and NIH3T3 cell lines were cultivated in BHK-21 and DME, respectively, which were supplemented with 10% FBS, L-glutamine (1% vol/vol), 10 U/ml penicillin, and 100 μg/ml streptomycin. The pci110 plasmid, which expresses ICP0, has been described previously (Everett et al., 1993). The wt strain HSV-1 syn+ (17+) is the parental strain (referred to as HSV-1 wt in this study). The dl1403 virus, which was deleted of ICP0 (Stow and Stow, 1986), the vFXE virus, which expresses a nonfunctional ICP0 isoform

mutated in its RING finger domain, and the standard infection procedures have been described previously (Everett, 1989).

Transfection, infection, IF, and confocal microscopy

Cells were seeded at 1.5×10^5 cells per well for transfection and at 2.5×10^5 cells per well for infection in 24-well plates that contained round coverslips. 24 h later, the cells were transfected with the pci110 plasmid according to the manufacturer's recommendations (Effectene Transfection Reagent; QIAGEN) or infected. Cells were treated for IF as described previously (Lomonte et al., 2001). With the exception of Fig. 5, in which a CCD camera (CoolSNAP HQ; Roper Scientific) was used for the analysis (Metaview software; Molecular Devices), all of the samples were examined under a confocal microscope (LSM 510 Meta; Carl Zeiss MicroImaging, Inc.). The data from the channels were collected separately to avoid channel overlap, with fourfold averaging at a resolution of 512×512 pixels using optical slices of 0.8–1.0-μm thickness. A microscope (Axiovert 200M; Carl Zeiss MicroImaging, Inc.) was used at either 63× (NA 1.25) or 100× (NA 1.3) magnification by oil-immersion objective lenses (Carl Zeiss MicroImaging, Inc.). Datasets were processed using LSM 510 software (Carl Zeiss MicroImaging, Inc.) and exported in preparation for printing using Photoshop (Adobe).

IF in situ hybridization

Immuno-RNA FISH. HeLa cells were seeded at 1.5×10^5 cells per well in 24-well plates that contained coverslips. The next day, the cells were transfected with the pci110 plasmid. After 24 h, the cells were rinsed in 1× PBS and fixed with 4% formaldehyde in 1× PBS for 10 min. The cells were rinsed again in 1× PBS and incubated overnight at 4°C in 70% ethanol. The cells were then rehydrated for 5 min in 2× SSC with 50% formamide and hybridized overnight at 37°C with 3 ng of the digoxigenin-labeled snRNA U2 probe (5′-ATACTGATAAGAACAGATACTACACTTGATCTTAGCCATA-3′) diluted in 40 μl of 2× SSC that contained 10% dextran sulfate, 2 mM vanadyl-ribonucleoside complex, 0.02% BSA (Rnase free), 40 μg *Escherichia coli* tRNA, and 50% formamide. 1 d later, the cells were washed twice for 30 min at 37°C in 2× SSC that contained 50% formamide and were then washed three times at 37°C with 1× PBS that contained 1% FBS. The cells were finally treated for IF to reveal proteins as described previously (Lomonte et al., 2001). An FITC-labeled sheep anti-digoxigenin antibody diluted 1:500 was used to reveal the probe.

Immuno-DNA FISH. Cells were first processed for immunostaining as indicated in the previous section and were postfixed with PFA and treated for FISH using the three-dimensional FISH procedure of Solovei et al. (2002) to ensure maximum preservation of the nuclear architecture. Probes were generated from the mouse major and minor satellite DNAs, which were obtained by PCR amplification of genomic DNA from the NIH3T3 cells used in this study using the following primers: for the major satellite MMS 24C, 5′-CATATTCCAGGTCCTTCAGTGTGC-3′; for MMS 24D, 5′-CACTTTAGGACGTGAAATATGGCG-3′; for the minor satellite MS 24C, 5′-ACTCATCTAATATGTTCTACAGTG-3′; and for MS box 1, 5′-AAAACACATTCGTTGGAAAC-GGG-3′. The major and minor satellite DNAs were labeled with either biotin-16-dUTP or digoxigenin-11-dUTP by nick translation (Roche Diagnostics). A standard procedure was used for probe detection using either AlexaFluor555-labeled streptavidin (Invitrogen) or FITC-labeled antidigoxigenin antibodies (Roche Diagnostics). Nuclear DNA was counterstained with Hoechst 33258, and the cells were mounted with Vectashield antifade.

ChIP and real-time PCR assays

Cells were seeded at 5×10^6 cells per 100-mm Petri dish. The following day, the cells were infected with the HSV-1 virus for 4 h and were subjected to the ChIP assay (Upstate Biotechnology). The samples were incubated with IgG Fab fragments (US Biological) before adding the test antibodies to decrease the nonspecific binding of alphoid DNA repeats to IgG. DNA that was immunoprecipitated with the different antibodies was quantified by PCR using specific primers. The PCR reaction was performed in a LightCycler (Roche Diagnostics) using 1 μl DNA, 0.5 μM of each primer, and 10 μl SYBR green (QIAGEN) in a final volume of 20 μl. The data were analyzed using the LightCycler software (Roche Diagnostics). The α-SAT and GAPDH designations indicate oligonucleotides that are specific for the centromeric type I α-SAT DNA and the gene that encodes the GAPDH enzyme, respectively. The α-SAT oligonucleotides were designed based on the consensus α-SAT sequence (Alexandrov et al., 1993), which was derived from the alignment of >500 type I alphoid sequences. Moreover, a BLAST search using this consensus type I α-SAT showed hits for cosmids from several chromosomes. Therefore, these oligonucleotides amplify DNA fragments from several different chromosomes, and the ChIP data are likely to reflect the association of proteins with several chromosome centromeres. The primers used were as follows: for α-SAT, forward 5′-AATCTGCAAGTGGATATTT-3′ and reverse 5′-CTACAAAAAGAGTGTTTCAAAAC-3′; for GAPDH, forward 5′-CACGTAGCTCAGGCCTCAAGA-3′ and reverse 5′-AGGCTGCGGGCTCAATTTAT-3′. The data shown are the ratios between the values obtained for the immunoprecipitated chromatin and the input DNA and are the mean values from six independent experiments.

siRNA transfections

HeLa cells were seeded at 4×10^4 cells per well in a 24-well plate that contained round coverslips for IF or at 1×10^6 cells per 60-mm Petri dish for WB. 1 d later, the cells were transfected with 300 ng (for IF) or 7 μg (for WB) siRNA that targets the mRNA of CENP-A, -B, or -C and were incubated for 48 h. A second round of siRNA transfection was performed as described above, and cells were incubated for an additional 48 h before the cells were harvested for IF or WB experiments. For WB, 40-μg aliquots of total protein were loaded per well in an SDS-polyacrylamide gel before electrophoresis, transfer, and detection as described previously (Lomonte et al., 2004). The siRNA sequences used were as follows: for *CENP-A*, 5′-GGUUGGCUAAAGGAGAUCCTT-3′; for *CENP-B*, 5′-CUACACCGCCAACUCCAAGTT-3′; and for *CENP-C*, 5′-GAAGCCUCUCUACAGUUUGTT-3′.

Antibodies

The following antibodies were used at the indicated dilutions for the IF, WB, or ChIP experiments: mAbs anti-p62 (TFIIH at 1:400 for IF), [3–19] anti–CENP-A (1 μg/ml for WB and 2 μg per sample for ChIP; Abcam), [5E6C1] anti–CENP-B (1 μg/ml for WB), anticoilin (1:400 for IF, 1 μg/ml for WB, and 2 μg per sample for ChIP; Sigma-Aldrich), [25–4] anti–DNA-PKcs (1:200 for IF; NeoMarkers); [72B9] antifibrillarin (1:500 for IF), [38F3] antifibrillarin (1:500 for WB; Abcam), anti–gemin 2 (1:200 for IF; Abcam), [12H12] anti–gemin 3 (1:200 for IF; Abcam), anti–HCF-1 (1:400 for IF), [11060] anti-ICP0 (1:1,000 for IF and 1:10,000 for WB), [8.F.137B] anti-ICP4 (1:100 for IF; US Biological), [9E10] anti-myc (2 μg per sample for ChIP; Abcam), [D0-7] anti-p53 (1:500 for IF; DakoCytomation), [5E10] anti–promyelocytic leukaemia (PML; 1:50 for IF), [51RAD01] anti-Rad51 (1:200 for IF; NeoMarkers), [9H8] anti-RPA32 (1:200 for IF; Abcam), Y12 anti-Sm (1:500 for IF; NeoMarkers), anti-SMN (1:400 for IF; 1 μg/ml for WB; BD Biosciences), and anti–2,2,7-trimethylguanosine (TMG at 1:300 for IF; Oncogene Research Products). In addition, the following rabbit polyclonal antibodies were used: antiactin (1 μg/ml for WB; Sigma-Aldrich), 1343 anti-BLM (1:500 for IF), anti–CENP-A (1:200 for IF; Upstate Biotechnology), anti–CENP-B (1:2,000 for IF), r554 anti–CENP-C (1:1,000 for IF and WB), rp80 anticoilin (1:400 for IF), anti-FLASH (1:4,000 for IF), anti-γH2AX (phospho-S139 at 1:500 for IF; Abcam), R190 anti-ICP0 (1:200 for IF), anti-PA28γ (N terminus; 1:200 for IF; Zymed Laboratories), and BL647 antiphospho-RPA32 (S4/S8 at 1:1,000 for IF; Bethyl Laboratories). The human autoimmune serum huACA against CENPs was also used (1:3,000 for IF). For IFs, the secondary antibodies used were as follows: goat anti–rabbit, anti–mouse, and anti–human antibodies coupled to AlexaFluor488, -555, or -647 (1:200; Invitrogen).

We thank the following people for donating materials: Mounira Amor-Guéret for anti-BLM (Institut Curie, Orsay, France), William R. Brinkley for CENP-B$^{-/-}$ cells (Baylor College of Medicine, Houston, TX), Jérome Cavaillé for mAb 72B9 (Université Paul Sabatier, Toulouse, France), Vincenzo De Laurenzi for anti-FLASH (Universita' di Roma, Rome, Italy), William Earnshaw for huACA, rabbit anti–CENP-B, and r554 (Institute of Cell and Molecular Biology, Edinburgh, Scotland, UK), Jean-Marc Egly for anti-p62 (Institut de Génétique et de Biologie Moléculaire et Cellulaire, Strasbourg, France), Roger Everett for mAb 11060 and R190 (Medical Reseach Council Virology Unit, Glasgow, Scotland, UK), Winship Herr for anti–HCF-1 (Center for Integrative Genomics, Lausanne, Switzerland), Jérome Lamartine for human keratinocyte primary cells (Centre de Génétique Moléculaire et Cellulaire/Université Claude Bernard Lyon 1), Angus Lamond for rp80 anticoilin (Wellcome Trust Biocenter, Dundee, Scotland, UK), Hiroshi Masumoto for mAb 5E6C1 and technical advice (Division of Biological Science, Nagoya University, Nagoya, Japan), and Roel van Driel for mAb 5E10 (University of Amsterdam, Amsterdam, Netherlands). We also thank Joëlle Thomas for her help with real-time PCR and constructive criticism of the manuscript and thank William Earnshaw for insightful comments.

This work was funded by the Centre National de la Recherche Scientifique through the Action Thématique Incitative sur Programme Young Researchers Program, the National Agency for Research (grant ANR-05-MIIM-008-01) through the CENTROLAT program, and the National Institute of Cancer through the EPIPRO program.

Submitted: 19 December 2006
Accepted: 2 May 2007

References

Alexandrov, I.A., L.I. Medvedev, T.D. Mashkova, L.L. Kisselev, L.Y. Romanova, and Y.B. Yurov. 1993. Definition of a new alpha satellite suprachromosomal family characterized by monomeric organization. *Nucleic Acids Res*. 21:2209–2215.

Barcaroli, D., D. Dinsdale, M.H. Neale, L. Bongiorno-Borbone, M. Ranalli, E. Munarriz, A.E. Sayan, J.M. McWilliam, T.M. Smith, E. Fava, et al. 2006. FLASH is an essential component of Cajal bodies. *Proc. Natl. Acad. Sci. USA*. 103:14802–14807.

Bharadwaj, R., and H. Yu. 2004. The spindle checkpoint, aneuploidy, and cancer. *Oncogene*. 23:2016–2027.

Blower, M.D., B.A. Sullivan, and G.H. Karpen. 2002. Conserved organization of centromeric chromatin in flies and humans. *Dev. Cell*. 2:319–330.

Blower, M.D., T. Daigle, T. Kaufman, and G.H. Karpen. 2006. *Drosophila* CENP-A mutations cause a BubR1-dependent early mitotic delay without normal localization of kinetochore components. *PLoS Genet*. 2:e110.

Bouzinba-Segard, H., A. Guais, and C. Francastel. 2006. Accumulation of small murine minor satellite transcripts leads to impaired centromeric architecture and function. *Proc. Natl. Acad. Sci. USA*. 103:8709–8714.

Cioce, M., and A.I. Lamond. 2005. Cajal bodies: a long history of discovery. *Annu. Rev. Cell Dev. Biol.* 21:105–131.

Cioce, M., S. Boulon, A.G. Matera, and A.I. Lamond. 2006. UV-induced fragmentation of Cajal bodies. *J. Cell Biol.* 175:401–413.

Cleveland, D.W., Y. Mao, and K.F. Sullivan. 2003. Centromeres and kinetochores: from epigenetics to mitotic checkpoint signaling. *Cell*. 112:407–421.

Collier, S., A. Pendle, K. Boudonck, T. van Rij, L. Dolan, and P. Shaw. 2006. A distant coilin homologue is required for the formation of cajal bodies in *Arabidopsis*. *Mol. Biol. Cell*. 17:2942–2951.

Everett, R.D. 1989. Construction and characterization of herpes simplex virus type 1 mutants with defined lesions in immediate early gene 1. *J. Gen. Virol.* 70:1185–1202.

Everett, R.D., A. Cross, and A. Orr. 1993. A truncated form of herpes simplex virus type 1 immediate-early protein Vmw110 is expressed in a cell type dependent manner. *Virology*. 197:751–756.

Everett, R.D., P. Freemont, H. Saitoh, M. Dasso, A. Orr, M. Kathoria, and J. Parkinson. 1998. The disruption of ND10 during herpes simplex virus infection correlates with the Vmw110- and proteasome-dependent loss of several PML isoforms. *J. Virol.* 72:6581–6591.

Everett, R.D., W.C. Earnshaw, J. Findlay, and P. Lomonte. 1999a. Specific destruction of kinetochore protein CENP-C and disruption of cell division by herpes simplex virus immediate-early protein Vmw110. *EMBO J.* 18:1526–1538.

Everett, R.D., W.C. Earnshaw, A.F. Pluta, T. Sternsdorf, A.M. Ainsztein, M. Carmena, S. Ruchaud, W.L. Hsu, and A. Orr. 1999b. A dynamic connection between centromeres and ND10 proteins. *J. Cell Sci.* 112:3443–3454.

Foltz, D.R., L.E. Jansen, B.E. Black, A.O. Bailey, J.R. Yates III, and D.W. Cleveland. 2006. The human CENP-A centromeric nucleosome-associated complex. *Nat. Cell Biol.* 8:458–469.

Fukagawa, T., M. Nogami, M. Yoshikawa, M. Ikeno, T. Okazaki, Y. Takami, T. Nakayama, and M. Oshimura. 2004. Dicer is essential for formation of the heterochromatin structure in vertebrate cells. *Nat. Cell Biol.* 6:784–791.

Gall, J.G. 2001. A role for Cajal bodies in assembly of the nuclear transcription machinery. *FEBS Lett.* 498:164–167.

Gall, J.G. 2003. The centennial of the Cajal body. *Nat. Rev. Mol. Cell Biol.* 4:975–980.

Guenatri, M., D. Bailly, C. Maison, and G. Almouzni. 2004. Mouse centric and pericentric satellite repeats form distinct functional heterochromatin. *J. Cell Biol.* 166:493–505.

Hagglund, R., and B. Roizman. 2004. Role of ICP0 in the strategy of conquest of the host cell by herpes simplex virus 1. *J. Virol.* 78:2169–2178.

Hebert, M.D., and A.G. Matera. 2000. Self-association of coilin reveals a common theme in nuclear body localization. *Mol. Biol. Cell*. 11:4159–4171.

Hudson, D.F., K.J. Fowler, E. Earle, R. Saffery, P. Kalitsis, H. Trowell, J. Hill, N.G. Wreford, D.M. de Kretser, M.R. Cancilla, et al. 1998. Centromere protein B null mice are mitotically and meiotically normal but have lower body and testis weights. *J. Cell Biol.* 141:309–319.

Jallepalli, P.V., and C. Lengauer. 2001. Chromosome segregation and cancer: cutting through the mystery. *Nat. Rev. Cancer*. 1:109–117.

Kapoor, M., R. Montes de Oca Luna, G. Liu, G. Lozano, C. Cummings, M. Mancini, I. Ouspenski, B.R. Brinkley, and G.S. May. 1998. The cenpB gene is not essential in mice. *Chromosoma*. 107:570–576.

Lefebvre, S., L. Burglen, S. Reboullet, O. Clermont, P. Burlet, L. Viollet, B. Benichou, C. Cruaud, P. Millasseau, M. Zeviani, et al. 1995. Identification and characterization of a spinal muscular atrophy-determining gene. *Cell*. 80:155–165.

Liu, Q., and G. Dreyfuss. 1996. A novel nuclear structure containing the survival of motor neurons protein. *EMBO J.* 15:3555–3565.

Lomonte, P., and R.D. Everett. 1999. Herpes simplex virus type 1 immediate-early protein Vmw110 inhibits progression of cells through mitosis and from G(1) into S phase of the cell cycle. *J. Virol.* 73:9456–9467.

Lomonte, P., and E. Morency. 2007. Centromeric protein CENP-B proteasomal degradation induced by the viral protein ICP0. *FEBS Lett.* 581:658–662.

Lomonte, P., K.F. Sullivan, and R.D. Everett. 2001. Degradation of nucleosome-associated centromeric histone H3-like protein CENP-A induced by herpes simplex virus type 1 protein ICP0. *J. Biol. Chem.* 276:5829–5835.

Lomonte, P., J. Thomas, P. Texier, C. Caron, S. Khochbin, and A.L. Epstein. 2004. Functional interaction between class II histone deacetylases and ICP0 of herpes simplex virus type1. *J. Virol.* 78:6744–6757.

Luciani, J.J., D. Depetris, Y. Usson, C. Metzler-Guillemain, C. Mignon-Ravix, M.J. Mitchell, A. Megarbane, P. Sarda, H. Sirma, A. Moncla, et al. 2006. PML nuclear bodies are highly organised DNA-protein structures with a function in heterochromatin remodelling at the G2 phase. *J. Cell Sci.* 119:2518–2531.

Maison, C., D. Bailly, A.H. Peters, J.P. Quivy, D. Roche, A. Taddei, M. Lachner, T. Jenuwein, and G. Almouzni. 2002. Higher-order structure in pericentric heterochromatin involves a distinct pattern of histone modification and an RNA component. *Nat. Genet.* 30:329–334.

Matera, A.G., and M.R. Frey. 1998. Coiled bodies and gems: Janus or gemini? *Am. J. Hum. Genet.* 63:317–321.

Matera, A.G., and K.B. Shpargel. 2006. Pumping RNA: nuclear bodybuilding along the RNP pipeline. *Curr. Opin. Cell Biol.* 18:317–324.

Morency, E., Y. Coute, J. Thomas, P. Texier, and P. Lomonte. 2005. The protein ICP0 of herpes simplex virus type 1 is targeted to nucleoli of infected cells. Brief report. *Arch. Virol.* 150:2387–2395.

Newton, K., E. Petfalski, D. Tollervey, and J.F. Caceres. 2003. Fibrillarin is essential for early development and required for accumulation of an intron-encoded small nucleolar RNA in the mouse. *Mol. Cell. Biol.* 23:8519–8527.

Ohzeki, J., M. Nakano, T. Okada, and H. Masumoto. 2002. CENP-B box is required for de novo centromere chromatin assembly on human alphoid DNA. *J. Cell Biol.* 159:765–775.

Okada, M., I.M. Cheeseman, T. Hori, K. Okawa, I.X. McLeod, J.R. Yates III, A. Desai, and T. Fukagawa. 2006. The CENP-H-I complex is required for the efficient incorporation of newly synthesized CENP-A into centromeres. *Nat. Cell Biol.* 8:446–457.

Omer, A.D., S. Ziesche, H. Ebhardt, and P.P. Dennis. 2002. In vitro reconstitution and activity of a C/D box methylation guide ribonucleoprotein complex. *Proc. Natl. Acad. Sci. USA*. 99:5289–5294.

Parkinson, J., S.P. Lees-Miller, and R.D. Everett. 1999. Herpes simplex virus type 1 immediate-early protein vmw110 induces the proteasome-dependent degradation of the catalytic subunit of DNA-dependent protein kinase. *J. Virol.* 73:650–657.

Perez-Castro, A.V., F.L. Shamanski, J.J. Meneses, T.L. Lovato, K.G. Vogel, R.K. Moyzis, and R. Pedersen. 1998. Centromeric protein B null mice are viable with no apparent abnormalities. *Dev. Biol.* 201:135–143.

Pidoux, A.L., and R.C. Allshire. 2005. The role of heterochromatin in centromere function. *Philos. Trans. R. Soc. Lond. B. Biol. Sci.* 360:569–579.

Pietras, D.F., K.L. Bennett, L.D. Siracusa, M. Woodworth-Gutai, V.M. Chapman, K.W. Gross, C. Kane-Haas, and N.D. Hastie. 1983. Construction of a small Mus musculus repetitive DNA library: identification of a new satellite sequence in Mus musculus. *Nucleic Acids Res.* 11:6965–6983.

Raska, I., L.E. Andrade, R.L. Ochs, E.K. Chan, C.M. Chang, G. Roos, and E.M. Tan. 1991. Immunological and ultrastructural studies of the nuclear coiled body with autoimmune antibodies. *Exp. Cell Res.* 195:27–37.

Rieder, C.L., and H. Maiato. 2004. Stuck in division or passing through: what happens when cells cannot satisfy the spindle assembly checkpoint. *Dev. Cell*. 7:637–651.

Saffery, R., H. Sumer, S. Hassan, L.H. Wong, J.M. Craig, K. Todokoro, M. Anderson, A. Stafford, and K.H. Choo. 2003. Transcription within a functional human centromere. *Mol. Cell*. 12:509–516.

Schueler, M.G., and B.A. Sullivan. 2006. Structural and functional dynamics of human centromeric chromatin. *Annu. Rev. Genomics Hum. Genet.* 7:301–313.

Shpargel, K.B., J.K. Ospina, K.E. Tucker, A.G. Matera, and M.D. Hebert. 2003. Control of Cajal body number is mediated by the coilin C-terminus. *J. Cell Sci.* 116:303–312.

Solovei, I., A. Cavallo, L. Schermelleh, F. Jaunin, C. Scasselati, D. Cmarko, C. Cremer, S. Fakan, and T. Cremer. 2002. Spatial preservation of nuclear

chromatin architecture during three-dimensional fluorescence in situ hybridization (3D-FISH). *Exp. Cell Res.* 276:10–23.

Stow, N.D., and E.C. Stow. 1986. Isolation and characterization of a herpes simplex virus type 1 mutant containing a deletion within the gene encoding the immediate early polypeptide Vmw110. *J. Gen. Virol.* 67:2571–2585.

Tanaka, Y., H. Tachiwana, K. Yoda, H. Masumoto, T. Okazaki, H. Kurumizaka, and S. Yokoyama. 2005. Human centromere protein B induces translational positioning of nucleosomes on alpha-satellite sequences. *J. Biol. Chem.* 280:41609–41618.

Topp, C.N., C.X. Zhong, and R.K. Dawe. 2004. Centromere-encoded RNAs are integral components of the maize kinetochore. *Proc. Natl. Acad. Sci. USA*. 101:15986–15991.

Tucker, K.E., L.K. Massello, L. Gao, T.J. Barber, M.D. Hebert, E.K. Chan, and A.G. Matera. 2000. Structure and characterization of the murine p80 coilin gene, Coil. *J. Struct. Biol.* 129:269–277.

Tucker, K.E., M.T. Berciano, E.Y. Jacobs, D.F. LePage, K.B. Shpargel, J.J. Rossire, E.K. Chan, M. Lafarga, R.A. Conlon, and A.G. Matera. 2001. Residual Cajal bodies in coilin knockout mice fail to recruit Sm snRNPs and SMN, the spinal muscular atrophy gene product. *J. Cell Biol.* 154:293–307.

Tuma, R.S., J.A. Stolk, and M.B. Roth. 1993. Identification and characterization of a sphere organelle protein. *J. Cell Biol.* 122:767–773.

Verdel, A., and D. Moazed. 2005. RNAi-directed assembly of heterochromatin in fission yeast. *FEBS Lett.* 579:5872–5878.

Wilk, S., W.E. Chen, and R.P. Magnusson. 2000. Properties of the nuclear proteasome activator PA28gamma (REGgamma). *Arch. Biochem. Biophys.* 383:265–271.

Yoda, K., S. Ando, A. Okuda, A. Kikuchi, and T. Okazaki. 1998. In vitro assembly of the CENP-B/alpha-satellite DNA/core histone complex: CENP-B causes nucleosome positioning. *Genes Cells*. 3:533–548.

Zhang, W., C. Yi, W. Bao, B. Liu, J. Cui, H. Yu, X. Cao, M. Gu, M. Liu, and Z. Cheng. 2005. The transcribed 165-bp CentO satellite is the major functional centromeric element in the wild rice species *Oryza punctata*. *Plant Physiol*. 139:306–315.